www.shd.org.rs

Journal of the Serbian Chemical Society

JSCS@tmf.bg.ac.yu • www.shd.org.rs/JSCS

J. Serb. Chem. Soc. 73 (8–9) 891–913 (2008)
JSCS–3771

UDC 546.26+539.24:621.315.59:519.17
Review paper

REVIEW

Carbon nanotubes

SLOBODAN N. MARINKOVIĆ*

Vinča Institute of Nuclear Sciences, P.O. Box 522, Belgrade, Serbia

(Received 14 March, revised 17 May 2008)

Abstract: Nanotubes, the last in the focus of scientists in a series of "all carbon" materials discovered over the last several decades are the most interesting and have the greatest potential. This review aims at presenting in a concise manner the considerable amount of knowledge accumulated since the discovery of this amazing form of solid carbon, particularly during the last 15 years. The topics include methods of synthesis, mathematical description, characterization by Raman spectroscopy, most important properties and applications. Problems related to the determination of CNT properties, as well as difficulties regarding their applications, in particular scaling, which would lead to their utilization, are outlined.

Keywords: carbon nanotubes; single-wall nanotubes; multi-wall nanotubes; intercalation; doping; graphene.

CONTENTS

* Correspondence: zmar@ptt.yu
doi: 10.2298/JSC0809891M

1. INTRODUCTION

Carbon is a versatile element and it can form various allotropes, including graphite, diamond and fullerene-like structures. In the well-known layered structure of graphite, there is a large difference in chemical bonding within the layers and between them. The σ-bonds connecting each C atom with its three neighbours within the layers are created by sp^2 hybridization. They are possibly the strongest existing chemical bonds. The remaining fourth, delocalized electron in graphite is responsible for the very weak π-bonds acting between the layers. It also determines the "semimetallic" character of graphite. The difference in the bond strength is reflected in the different bond distances: 0.142 nm between the neighbouring C atoms within the layers, as opposed to 0.335 nm between the layers. Due to the large difference in the bond strength, the layers behave in a rather "independent" way and are termed "graphene" layers.

With the study of C_{60} and C_{70}, it was soon realized that an infinite variety of closed graphitic structures could be formed, each with unique properties. All that was necessary to create such a structure was to have 12 pentagons present to close the hexagonal network (as explained by the Euler theorem). Since C_{70} was already slightly elongated, tubular fullerenes were imagined.

However, carbon nanotubes were discovered long before researchers even imagined that carbon may exist in such a form. It was in 1952 when Radushkevich and Lukyanovich reported the discovery of "worm-like" carbon formations.[1] These were observed during their study of the soot formed by decomposition of CO on iron particles at 600 °C. On the basis of many experiments and TEM images, the authors conclude that the formed product consisted of long filamentary or needle-like carbon crystals with diameters of about 50 nm (the narrowest seen in their TEM images were about 30 nm), probably hollow, growing from iron compound (probably carbide) particles. In other words, the products were carbon nanotubes. The discovered carbon nanotubes (CNTs), as we know today, were in fact multi-walled (MWNTs), but the resolution of their TEM was too low (5–6 nm) to enable the authors to see the arrangement of graphenes in the nanotube walls. It is interesting that the authors also found couples of intertwined nanotubes, resembling at the first sight the DNA double helix structure.

The discovery of nanotubes passed almost unnoticed, like a number of other studies before and after it.[2]

In 1991, researchers at the Naval Research Laboratory first predicted that by simply turning a graphene sheet into a small tube, the structure would at room temperature have a carrier density similar to that of metals and zero band gap, unlike graphite.[3]

Simultaneously, the experimental work of Iijima[4] led to what is wrongly thought today by a majority of researchers to be the first discovery of carbon nanotubes (CNTs), more specifically multiwalled nanotubes (MWNTs). When exa-

mining fullerene soot, Iijima also examined parts of the graphite electrodes of the arc generator and the graphite rod that served as a cathode and found surprisingly regular needle-like structures. A closer examination revealed that each needle consisted of several concentrically arranged seamless graphene tubes, regularly separated by about 0.34 nm spaces, the distance between layers in graphite (Fig. 1). Electron diffraction performed by TEM on individual needles revealed that the tubules seem to consist of rolled up graphene layers. Each tubule appeared to be rolled up in a different fashion, *i.e.*, it exhibited different helicity (instead of "helicity", the term "chirality" is preferred by a number of authors). The different degrees of helicity in each shell are necessary to obtain the best fit between the successive shells in a tube and minimize the interlayer distance.[5] The nanotubes, which could extend in length up to many micrometers, were closed at the end by a half-spherical or faceted cap (the caps consisted of both hexagons and pentagons) and thus resembled extremely elongated, large diameter fullerenes. This paper was the first unambiguous evidence for the possibility of growing carbon nanotubes without the need of any catalyst. It was the work of Iijima that produced a worldwide explosion of research on carbon nanotubes.

The formation of single-wall nanotubes (SWNTs) was first reported in 1993 by two papers submitted independently.[6,7] A sketch of a SWNT with caps at both ends is shown in Fig. 2.

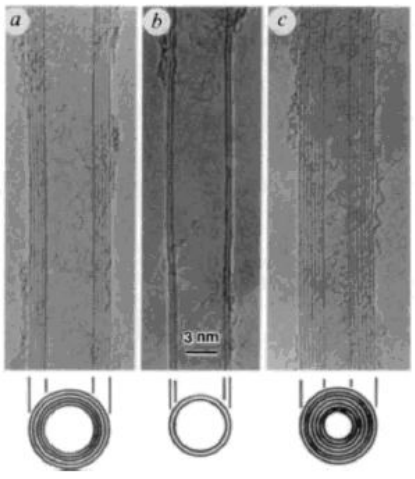

Fig. 1. Electron micrographs of carbon nanotubes. Parallel dark lines correspond to the (002) lattice images of graphite. A cross-section of each nanotube is illustrated: a) a tube consisting of five graphitic sheets, diameter 6.7 nm, b) A two-sheet tube, diameter 5.5 nm and c) A seven-sheet tube, diameter 6.5 nm, which has the smallest hollow diameter (2.2 nm).[4] (Reprinted with permission from Macmillan Publishers Ltd.).

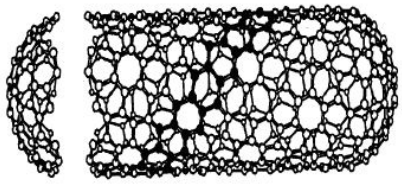

Fig. 2. Sketch of the structure of a single-wall nanotube with caps at both ends. The tube has helicity as indicated by the black coloured carbon atoms forming a screw-like array of hexagons.[8] (Reused with permission. Copyright 2000, American Institute of Physics).

Since the diameter of SWNTs can be as small as 0.4 nm with only 10 atoms around the circumference and the tubes can be only one atom in thickness, the aspect ratio (length-to-diameter) can be very large (>10^4), thus leading to a prototype one-dimensional (1D) system. In addition, depending on their diameter and helicity, CNTs are either one-dimensional metals or semiconductors. Therefore, they can be used to form metal-semiconductor, semiconductor-semiconductor, or metal–metal junctions.

The prospects of using CNTs in electronics and other fields led many researchers to study them, both experimentally and theoretically. In this review, the current knowledge on both pure and doped carbon nanotubes will be presented

2. SYNTHESIS OF CARBON NANOTUBES

Pure carbon nanotubes (CNTs), as well as B- or N-doped CNTs, can be synthesized using conditions far from equilibrium. Other dopants have been far less studied. The effect of substitutional Si atoms has recently been calculated. A number of authors deal with intercalation (insertion between neighbouring graphene layers in MWNTs, or between SWNTs in a bundle) of alkali metals, mainly K,[10–15] Li[10,16,17] and Rb,[13] but other dopants ($FeCl_3$,[12] Ba[18]), as well as La[11] and halogens (I,[19–23] Br[19]) as endohedral dopants (within the nanotube) have also been considered. Monthioux[24] gives an overview of intercalation into SWNTs.

Although there are now several methods for making nanotubes, the carbon arc method remains the most practical for scientific purposes and yields the most highly graphitized tubes, simply because the process uses a very high temperature (4000 K). The significance of properly graphitized CNTs is that only with such materials can one expect to find any correlation between theory and experiment.

2.1. Arc method

CNTs can be grown on the carbon cathode used in the d.c. arc discharge evaporation of carbon in an argon-filled vessel (100 torr).[4] The deposit generated has a hierarchical structure, with nanotubes organized in small bundles, which are themselves organized into 50 μm fibres visible to the eye. The alignment of the nanotubes along the axis of the arc current, the yield of the nanotubes and their structural quality all depend on the conditions of the arc. The most critical parameters are the inert gas pressure, the growth rate, the cooling rate, the stability of the plasma and some other variables difficult to quantify. Nanotube yields of about 60 % of the core material are obtainable under optimal conditions.[25]

The growth mechanism of nanotubes is a complex and fascinating subject. One of the first questions is why elongated structures such as nanotubes (and not balls) form although they are not thermodynamically stable. This seems to be the result of a competition between two types of carbon species present near the cathode surface, namely the anisotropic unidirectional carbon ions accelerated

across the gap, and the thermally evaporated carbon from the cathode with an isotropic velocity distribution. In other words, the introduction of an axis of symmetry in the reaction zone due to the unidirectional carbon species results in elongated structures. Analysis shows that an axis of symmetry always exists in all the methods used to generate nanotubes. For instance, in the catalytic growth of SWNTs, the catalytic particles provide this asymmetry in three dimensions.[5]

The early structures were all multi-wall nanotubes. Single-wall nanotubes with small (≈ 1 nm) and uniform diameters were synthesized simultaneously in 1993 by two research teams using arc-discharge methods with transition metal catalysts.[6,7] Crystalline ropes of SWNTs, with each rope containing tens to hundreds of tubes of approximately the same diameter, were synthesized in this early work. Subsequently, SWNTs have been synthesized by a number of researchers using the arc-discharge method.

The double-walled NT (DWNTs) occupy a somewhat special position because the interactions between the inner and the outer tube are very weak, thus making the possibility of performing studies of the individual constituents of the DWNTs at the single nanotube level. In addition, while retaining very similar morphology and properties as SWNTs, chemical reactivity of DWNTs is significantly different. This is particularly important when functionalization *(i.e.*, grafting of chemical functions at the CNT surface) is required to modify properties of the CNT.

B-doped MWNTs can be produced by arcing either BN/graphite or B/graphite electrodes in an inert atmosphere (*e.g.*, He, N_2). Large quantities of crystalline and long (≤ 100 μm) MWNTs are obtained. They contain 20–30 sheets and usually have ill-formed caps. It has proved difficult to produce B-doped SWNTs using this technique because B may obstruct the growth of the tubules under the extreme conditions.[26]

Arc experiments using pure graphite electrodes in NH_3 indicate that it is difficult to produce N-doped SWNTs and MWNTs, possibly because N_2 molecules are easily created and do not react with carbon. However, Glerup *et al.*[27] have recently demonstrated that it is possible to grow N-doped SWNTs by arcing composite anodes containing graphite, melamine, Ni and Y. The tubes exhibit a low (≤ 1 %) N concentration, and are sometimes corrugated.

2.2. Laser ablation

Pure SWNTs were produced in yields of more than 70 % by condensation of a laser-vaporized carbon–nickel–cobalt mixture.[28]

Zhang *et al.*[29] reported that sandwich-like C-BN nanotubes could be produced by laser vaporization of graphite-BN targets. Evidence for the existence of BC_7N layers within the MWNTs was reported. More recently, Gai *et al.*[30] demonstrated that B-doped SWNTs could be generated using laser vaporization of B-graphite–Co–Ni targets. The authors performed laser ablation experiments in-

side a silica tube placed in a furnace operating at 1100 °C under an Ar atmosphere at ≈ 500 torr. A laser beam (1064 nm, 10 Hz) was used to ablate a target composed of a carbon paste mixed with a Co:Ni catalyst and elemental B. SWNTs were found in the products when the B content in the target material was < 3 at. %, but with no detectable boron was present in the SWNTs. Higher B concentration resulted mostly in a mixture of graphite and metal encapsulated particles, the quantity of SWNTs being low.

Recently, Borowiak-Palen and co-workers[31] reported the production of B-doped SWNTs with higher concentrations of B, in which 15 % of the C atoms were replaced by B. These experiments were conducted by heating B_2O_3 in the presence of pure carbon SWNTs and NH_3 at 1150 °C. Further studies on these samples should be performed because the reported amount of B is too high compared to the solubility of B in graphite and MWNTs (< 2 wt % B).

2.3. Chemical vapour deposition (CVD)

CVD Synthesis of undoped CNTs is relatively easy. Both SWNTs and MWNTs can be grown by decomposing an organic gas over a substrate covered with metal catalyst particles. Nanotubes grow at the sites of the metal catalyst. Their synthesis on a relatively large scale was reported by the catalytic decomposition of hydrocarbons at 1200 °C using a floating catalyst method. The SWNTs were self-organized in rope-like bundles. Thiophene addition was found to promote the growth of the SWNTs and increase the yields of both SWNTs and MWNTs.[32] In a recent work,[33] the activity and lifetime of the catalysts were enhanced by water, thus allowing massive growth of super dense and vertically aligned nanotube "forests" with heights up to 2.5 mm, which could be easily separated from the catalysts, providing nanotube material with carbon purity above 99.98 %. The approach is applicable to other synthesis methods developed for the mass production of SWNTs.

Another approach considered to offer potential for the synthesis of carbon nanotubes (SWNTs in particular) in large quantities at significantly lower cost than that of other methods is the use flames, such as a premixed oxygen–acetylene–argon flame, with $Fe(CO)_5$ vapour as the source of the metallic catalyst.[34]

Various CVD methods have been used to synthesize N-containing CNTs. N-doped MWNTs were produced by: the thermal decomposition of N-containing hydrocarbons over Fe, Co and Ni; the pyrolysis of aminodichlorotriazine over laser-etched Co films at 1050 °C; the pyrolysis of melamine, which resulted in an increased N content (< 7 %) within corrugated tubular structures; the pyrolysis of melamine over laser-etched Fe, resulting in high yields of aligned $C_{13}N_x$ ($x < 1$) nanotubes/nanofibres (< 100 nm outer diameter, < 60 μm long); the pyrolysis of pyridine and methylpyrimidine, resulting in CN_x nanotubes with low N concentrations, which were easily oxidized compared to pure CNTs.[26]

The results showed that it is extremely difficult to generate crystalline and highly ordered structures containing large concentrations of N within a hexagonal carbon network. The degree of perfection strongly depends on the N concentration, the lower the N concentration, the more graphitic and the straighter are the nanotubes.

Of the various means for nanotube synthesis, CVD shows the most promise for industrial scale deposition in terms of its price/unit ratio. In addition, CVD is capable of growing nanotubes directly on a desired substrate, unlike the other mentioned methods. The growth sites are controllable by careful deposition of the catalyst. The CVD technique has the potential for enabling the large-scale production of nanotubes, as well as the growth of nanotubes at specific sites on microfabricated chips or at the tips of scanning probe microscopes. However, a lot of work remains to be done in this area in order to control the B or N content, as well as the nanotube structure.

3. MATHEMATICAL DESCRIPTION OF CARBON NANOTUBES

A SWNT can be mathematically described as a single graphene layer rolled up into a seamless cylinder, one atom thick, usually with a small number (perhaps 10–40) of C atoms around the circumference, and a great length (microns) along the cylinder axis. A carbon nanotube is specified by the chiral vector $\boldsymbol{C}_h$:

$$\boldsymbol{C}_h = n\boldsymbol{a}_1 + m\boldsymbol{a}_2 \quad (1)$$

where (n,m) are the pair of indices that denote the number of unit vectors $n\boldsymbol{a}_1$ and $m\boldsymbol{a}_2$. As shown in Fig. 3, the chiral vector $\boldsymbol{C}_h$ makes an angle θ, the chiral angle, with the so-called zigzag or $\boldsymbol{a}_1$ direction. The vector $\boldsymbol{C}_h$ connects two crystallographically equivalent sites O and A on a two-dimensional graphene sheet where a carbon atom is located on each vertex of the honeycomb structure. The axis of the zigzag nanotube ($m = 0$) corresponds to $\theta = 0°$, whereas the so-called armchair nanotube (for $n = m$) corresponds to $\theta = 30°$ and the nanotube axis for so-called chiral nanotubes (all other CNTs) corresponds to $0 < \theta < 30°$. The seamless cylinder joint of the nanotube is made by joining the line AB' to the parallel line OB in Fig. 3. The nanotube diameter d_t can be written in terms of the integers (n,m) as:

$$d_t = \boldsymbol{C}_h/\pi = a(m^2 + nm + n^2)^{1/2}/\pi \quad (2)$$

where $a = 1.42\times\sqrt{3}$ Å and corresponds to the lattice constant of the graphite sheet (the C–C distance is 1.42 Å).

The chiral angle θ is defined as $\theta = \tan^{-1}[\sqrt{3}m/(m + 2n)]$. Thus, a nanotube can be specified by either its (n,m) indices or equivalently by d_t and θ.

To define the unit cell for a one-dimensional nanotube, the vector OB in Fig. 3 is defined as the shortest repeat distance along the nanotube axis, thereby defining the translation vector $\boldsymbol{T}$:

$$\boldsymbol{T} = t_1\boldsymbol{a}_1 + t_2\boldsymbol{a}_2 \tag{3}$$

where the coefficients t_1 and t_2 are related to (n,m) by:

$$t_1 = (2m + n)/d_R$$
$$t_2 = -(2n + m)/d_R \tag{4}$$

where d_R is the greatest common divisor of $(2m + n, 2n + m)$ and is given by:

$$d_R = \begin{cases} d & \text{if} \quad n - m \text{ is not a multiple of } 3d \\ 3d & \text{if} \quad n - m \text{ is a multiple } 3d, \end{cases} \tag{5}$$

where d is the greatest common divisor of (n,m). The magnitude of the translation vector $\boldsymbol{T} = |\boldsymbol{T}| = \sqrt{3}L/d_R$, where L is the length of the chiral vector $\boldsymbol{C}_h = \pi d_t$ and d_t is the nanotube diameter. The unit cell of the nanotube is defined as the area delineated by the vectors $\boldsymbol{T}$ and $\boldsymbol{C}_h$. The number of hexagons, N, contained within the one-dimensional unit cell of a nanotube is determined by the integers (n,m) and is given by:

$$N = 2(m^2 + n^2 + nm)/dR \tag{6}$$

Thus, assuming 0.142 nm as the value of the C–C distance, $d_t = 1.36$ nm and $N = 20$ are obtained for a (10,10) nanotube.

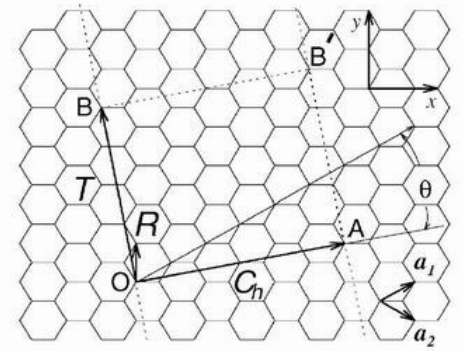

Fig. 3. a) The unrolled honeycomb lattice of a nanotube. When sites O and A, and sites B and B' are connected, a nanotube can be constructed. The vectors OA and OB define the chiral vector $\boldsymbol{C}_h$ and the translational vector $\boldsymbol{T}$ of the nanotube, respectively. The rectangle OAB'B defines the unit cell of the nanotube. The figure is constructed for an $(n,m) = (4,2)$ nanotube.[35] (Reprinted with permission from authors and publisher. Copyright 2004 by Annual Reviews, http://www.annnualreviews.org).

4. CHARACTERIZATION AND PROPERTIES OF CARBON NANOTUBES

The most important methods used to characterize CNTs are Raman spectroscopy, scanning electron microscopy (SEM), transmission electron microscopy (TEM), in particular High Resolution TEM (HRTEM), and scanning tunnelling microscopy (STM). Raman spectroscopy is capable of characterizing CNT samples, but it also provides detailed information on the vibrational modes of SWNTs and reveals a variety of unique phenomena in one-dimensional systems. Only Raman spectroscopy will be considered in this review.

4.1. Raman spectroscopy

The Raman spectra were taken with laser excitation energy E_{laser} = 2.41 eV (514.5 nm wavelength) for a SWNT bundle with diameter distribution of 1.36±0.20 nm (Fig. 4). They exhibit only two dominant features, namely, the radial breathing mode (RBM) out-of-plane vibrations, at 186 cm^{-1}, and the tangential (in-plane vibrations) band in the range from 1520–1620 cm^{-1} (Fig. 4, inset). Because of the strong connection of this tangential band to the corresponding mode in two-dimensional graphite, this higher frequency band for SWNTs is commonly called the G-band. Other lower intensity features, discussed below, also provide important and unique information about SWNTs.

The Raman spectra of SWNTs strongly and non-monotonously depend on the laser excitation energy, E_{laser}, and are associated with a resonance process for this energy with the optical transition energy between van Hove singularities in the valence and conduction bands.[36]

The results of Raman scattering studies on SWNTs[36] reveal not only many of the characteristic normal vibrational modes of a carbon nanotube, but also show that the Raman excitation frequency can be chosen to excite preferentially nanotubes of a particular diameter.

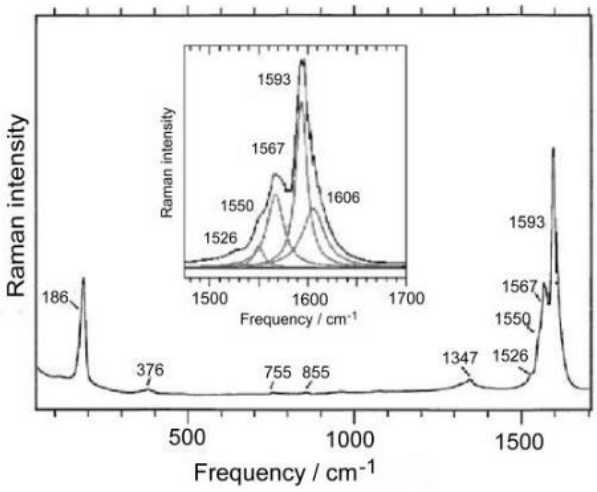

Fig. 4. The Raman spectrum taken with 514.5 nm (2.41 eV) laser excitation of a SWNT bundle sample with a diameter distribution d_t = 1.36±0.20 nm. The inset shows an expanded view of the spectra in the 1480–1700 cm^{-1} range.[36] (Reprinted with permission from AAAS.).

Figure 4 indicates that the G-band for SWNTs consists of two features: one peaking at 1593 cm^{-1} (G^+) and the other at 1567 cm^{-1} (G^-). The G^+ feature is associated with carbon atom in-plane vibrations along the nanotube axis and its frequency, ω_{G^+}, is sensitive to charge transfer from dopant additions to the SWNTs (up-shifts in ω_{G^+} for acceptors and downshifts for donors). In contrast, the G^- feature is associated with in-plane vibrations of carbon atoms along the circumferential direction of the nanotube and its line-shape is highly sensitive to whether the SWNT is metallic or semiconducting.[29] Also the D-band feature in

Fig. 4 with ω_D at 1347 cm^{-1} is commonly found in the Raman spectra of SWNT bundles, stemming from the disorder-induced mode in graphite. Its second harmonic, the G'-band (not shown), occurring at $\approx 2\omega_D$, is associated with a double resonance process.[35] Both the D-band and the G'-band are sensitive to the diameter and helicity of a nanotube.

Jorio[37] stated that the Raman scattering technique could provide complete structural information for 1-D systems, such as carbon nanotubes. Due to the sharp van Hove singularities occurring in carbon nanotubes with diameters less than 2 nm (see Fig. 7), the Raman intensities for the resonance Raman process can be so large that it is possible to observe the Raman spectra from one individual SWNT. The isolated SWNTs were prepared by a chemical vapour deposition method on an oxidized Si substrate containing nanometre-sized iron catalyst particles. The helicity of an (n,m) individual single-wall nanotube can be assigned uniquely by measuring one radial breathing mode frequency ω_{RBM} and using the theory of resonant transitions. A unique helicity assignment can be made for both metallic and semiconducting nanotubes.[37] The differences in the G-band spectra between semiconducting and metallic SWNTs are shown in Fig. 5.

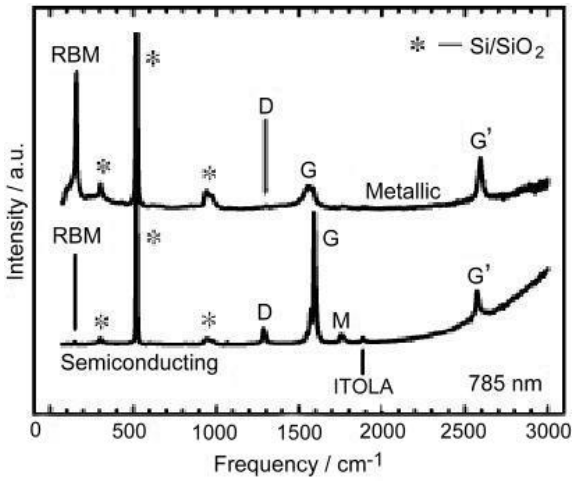

Fig. 5. Raman spectra from a metallic (top) and a semiconducting (bottom) SWNT at the single nanotube level, showing the radial breathing mode (RBM), D-band, G-band, and G'-band features, in addition to weak double resonance features (785 nm (1.58 eV) laser).The silicon substrate provides contributions to the Raman spectra, denoted by ∗.[35] (Reprinted with permission from authors and publicsher. Copyright 2004 by Annual Reviews, http://www.annnualreviews.org).

Measurements on the G-band at the single nanotube level show that this feature is a first-order process, with the frequency ω_{G^+} essentially independent of d_t or chiral angle θ, while ω_{G^-} is only dependent of d_t and not on θ. Such diameter dependent measurements can be done only at the single nanotube level.[37]

Raman spectra of carbon nanotubes, particularly at the single nanotube level, have been particularly rich in information. Due to the simplicity of the geometrical structure of nanotubes, detailed analysis of the Raman spectra has yielded a lot of information about phonon dispersion relations, such as information about their trigonal warping. This information was, in fact, not yet available for two-di-

mensional graphite but could be studied in nanotubes because of their one-dimensionality.[38] Thus, studies on carbon nanotubes are revealing a lot of important information about the electrons and phonons in 2-D graphite through studies at the single nanotube level, where the orientation of the wave vector can be explicitly probed, in contrast to the situation in 2-D graphite, which only allows measurements to be made as a function of the magnitude of the wave vector.[38]

4.2. Electronic properties

The nanometre dimensions of carbon nanotubes together with the unique electronic structure of a two-dimensional graphene sheet make the electronic properties of these one-dimensional carbon nanotube structures highly unusual.

The theory was ahead of experiment as far as the electronic properties of CNTs are concerned. Early theoretical calculations showed that the electronic properties of the carbon nanotubes are very sensitive to their geometric structure.[26] While graphene sheet is a zero-gap semiconductor in which the π-electrons propagate in all directions (2-dimensionally), theory has predicted that carbon nanotubes, where the electrons propagate only along the tube axis, can be either metals or semiconductors with different size energy gaps, depending very sensitively on the diameter and helicity of the tubes, *i.e.*, on the indices (*n*,*m*). The physics behind this sensitivity of the electronic properties of carbon nanotubes to their structure can be understood within the zone-folding picture.

If $n–m = 3j$, where j is an integer, the SWNTs are metallic*. On the other hand, all SWNTs with $n–m = 3j\pm1$ are large-gap (< 1.0 eV for $d_t < 0.7$ nm) semiconductors. Thus, for a uniform distribution of (*n*,*m*) values, there is a one-in-three chance of a SWNT being a metal and a two-in-three chance of it being a semiconductor.

These unique electronic properties arise from the quantum confinement of the electrons normal to the nanotube axis. In the radial direction, the electrons are confined by the monolayer thickness of the graphene sheet (≈ 0.350 nm).

Sufficiently strong hybridization effects between the σ and π states can occur through tube curvature effects in small-diameter nanotubes and these hybridization effects significantly alter their electronic structure. For example, a (5,0) tube, which is predicted to be semiconducting (see above), has been shown to be metallic by *ab initio* calculations.[35] Unusual properties have also been found in ultra-small diameter SWNTs ($d_t \approx 0.4$ nm), produced by confining their synthesis to occur inside zeolite channels.[39] This nanotube is the narrowest attainable that can still remain energetically stable, as predicted by theory. These ultra-small

* Strictly speaking, due to tube curvature effects, a tiny band gap opens up when j is not 0. However, for most experimentally observed carbon nanotubes, the gap would be so small that, for most practical purposes, all the $n–m = 3j$ tubes can be considered as metallic at room temperature because their thermal energy is sufficient to excite electrons from the valence to the conduction band.

diameter SWNTs have been reported to exhibit a variety of unusual properties for an all-carbon system, such as superconductivity.[40] The unit cell for such ultra-small diameter SWNTs is small enough to permit detailed and accurate *ab initio* calculations of their electronic structures.

Carbon nanotubes often have defects, such as pentagons, heptagons, vacancies or dopants, that drastically modify their electronic properties, which are, of course, more complex than those for infinitely long, perfect nanotubes. On the other hand, the introduction of defects into the carbon network is an interesting way to tailor its intrinsic properties to create new potential nanodevices and to propose new potential applications for nanotubes in nano-electronics.

The differences between the doped graphene sheet and CNT have been calculated.[41] Doping of a graphene sheet with 0.5 % B or N provokes a slight increase and shift in the electronic states close to the Fermi level (E_f), B (electron acceptor) in the valence band and N (electron donor) in the conduction band. Thus, density of states (DOS) *vs*. energy curves for a pure (undoped) and doped graphene sheets are quite similar to each other (Fig. 6). However, corresponding curves for doped and undoped nanotubes are quite different (Fig. 7). Because of the quantum confinement in the CNTs, being a consequence of their nanometer dimensions, the resulting number of 1-D conduction and valence bands effectively depends on the standing waves set-up around the circumerence of the nanotube. The spikes are called "van Hove" singularities and are typical of 1-D quantum conduction, which is not present in an infinite graphite crystal.

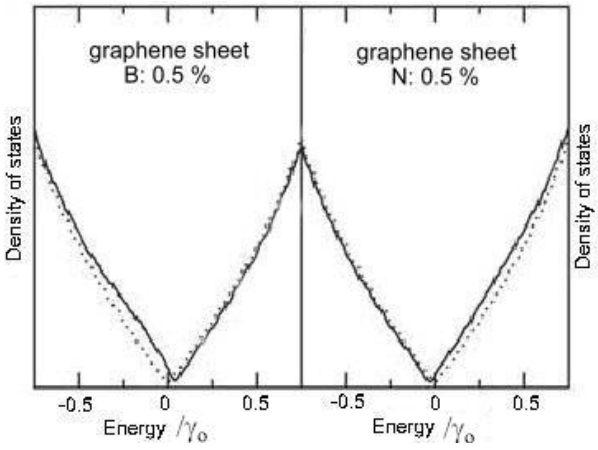

Fig. 6. DOS for doped and undoped graphene sheets (solid and dotted curves, respectively) (Terrones *et al.*[26] on the basis of results of Latil *et al.*[41]) (Reprinted with permission. Copyright Elsevier (2004).).

Little work has been performed on doping SWNTs with either B or N. However, it is believed that these systems should exhibit unusual quantum effects and it should be possible to tailor the band gaps of semiconducting SWNTs when doping at very low concentration levels. It should be pointed out that, in order to observe genuine quantum effects in doped CNTs, the dopants must be present within SWNTs of narrow diameter (< 1–2 nm).[26]

In N-doped SWNTs, N could be present substitutionally (N coordinated to three C atoms in an sp^2-like fashion), or as a pyridine-type N (two coordinated N), which can be incorporated into the SWNT, provided that a C atom is removed from the framework. This type of defect induces localized states below and above the Fermi level. Therefore, substitutional N doping in SWNTs should result in *n*-type conducting behaviour, whereas pyridine-type N may produce either a *p*- or *n*-type conductor, depending on the doping level, the number of N atoms, and the number of removed C atoms within the hexagonal sheet.

In experiments on simultaneous doping of SWNTs, bundles of B- and N-doped single-walled carbon nanotubes (SWNTs) containing up to ≈ 10 at. % B and up to ≈ 2 at. % N were synthesized at high yields under thermochemical treatment of pure carbon SWNT bundles and B_2O_3 in a flowing nitrogen atmosphere.[42]

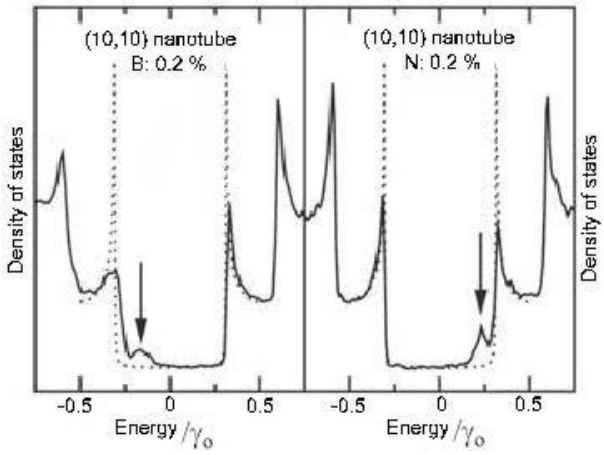

Fig. 7. DOS for doped and undoped metallic CNTs (solid and dotted lines, respectively). Note the peaks in the curves for the doped CNTs (arrows) in the valence band (B) and conduction band (N) (Terrones *et al.*[26] on the basis of results of Latil *et al.*[41]). (Reprinted with permission. Copyright Elsevier (2004).).

The amphoteric character of SWNTs, *i.e.*, their ability to exchange electrons with a dopant atom (or molecule) to form the corresponding positively or negatively charged counterion, has been shown also for the SWNTs exposed to typical electron-donor (potassium, rubidium) and electron-acceptor (iodine, bromine) dopants.[19]

Intercalation of single-wall carbon nanotubes (SWNTs) provides an important tool to modify their electronic band structure. In a particular case of the relatively large iodine ions, the size of SWNTs and the size of iodine are comparable. A commercial material used in the work of Grigorian *et al.*[20] comprised predominantly (6,5) and (7,5) nanotubes with diameters d_t = 0.757 and 0.829 nm, respectively. Taking into account the thickness of the nanotube wall (≈ 0.350 nm), the inner diameters d_{in} were 0.407 and 0.479 nm, respectively. The diameter of the iodine ions (d_I = 0.432 nm) is between these two values. Therefore, larger SWNTs with iodine-filled interiors were found to carry significantly higher charge density as compared to smaller empty ones.[20]

According to recent calculations,[9] silicon substitutional doping of SWNTs can dramatically change the local atomic and electronic structures of the SWNT at the doping site, which results in its preference to form sp^3 bonding, and the band structure of the doped SWNT exhibits a very different characteristic from that of the pristine SWNT. For the (5,5) tube, the metallic band structure can be changed into a doped degenerated semiconducting band structure with a distinct band gap and an unoccupied impurity band above the Fermi level. In addition, due to the formation of sp^3 bonds, the doping silicon atom can improve the local reaction activity of the tube.

4.3. Mechanical properties

Since the carbon–carbon chemical bond in a graphene layer is probably the strongest chemical bond known in nature (the sp^2 bond in graphite is stronger than the sp^3 bond in diamond), carbon nanotubes are expected to have exceptionally good mechanical properties, with significant potential for applications in the reinforcement of composite materials.

Some of the important parameters characterizing the mechanical properties of carbon nanotubes include their elastic constants, Young's modulus, Poisson ratio, response to deformation in the elastic regime, tensile and compressive strains, yield mechanism and strength at failure, toughness, and buckling when bent. One of the unusual features of nanotubes is that they simultaneously combine widely varying length scales: their length can be macroscopic, up to millimetres, whereas their diameters are on the nanoscale.

The manipulation of nanoscale objects is a difficult and challenging task. Nevertheless, a number of direct experimental measurements of the Young's modulus, Y, of nanotubes have appeared in the literature. Calculations show that the Young's modulus of isolated SWNTs does not depend greatly on the nanotube diameter or chiral angle and has a value of approximately 1 TPa, corresponding to the asymptotic limit reported for carbon fibres,[35] whereas Y for MWNTs decreases somewhat with increasing d_t. Despite the very high Young's modulus for carbon nanotubes, atomic force microscopy (AFM) measurements[43] indicate that nanotubes can bend into loops without breaking, testifying to their flexibility, toughness, and capacity for reversible deformation. Small-diameter SWNTs can be elongated by ≈ 30 % before breaking,[41] and values for the breaking strength of 55 GPa have been reported.[44] Tensile strength experiments performed on MWNTs showed that they break at the outermost layer, with the inner layers being pulled out like a sword from its sheath, and somewhat smaller values for the tensile strength were found for MWNTs.[44]

Under bending stress, MWNTs bend by stretching in the outer arc and by compression in the inner arc. For nanotubes with diameters $d_t < 12$ nm, the effective bending modulus was found to have a value of approximately 1 TPa.[45]

However, for MWNTs of larger diameters, the effective bending modulus drops dramatically to values of approximately 100 GPa. From these experiments, it was concluded that MWNTs, although difficult to stretch axially, are easy to bend laterally and they could reversibly withstand large lateral distortions.

Determining the actual strength of nanotubes from simulation is a challenging task. Atomistic calculations indicate that chiral tubes have a lower yield strain than either zigzag or armchair nanotubes,[35] which lowers their mechanical strength.

Concerning doped CNTs, the mechanical properties should not be substantially altered if the dopant concentration is low (*e.g.*, < 0.5 % N).[26]

Hernández and co-workers have calculated the mechanical properties of CN_x and CB_x nanotubes. Their results predict that of all the types of nanotubes considered (pure and doped), pure carbon nanotubes have the highest Young's modulus, approaching those of flat graphene-like sheets. They demonstrated that, although high concentrations of B and/or N within SWNTs lower the Young's modulus, the values still remain in the order of 0.5–0.8 TPa.[46,47]

However, the experimental values are quite different from the theoretical ones. For example, the Young's moduli for pristine and N-doped MWNTs are 0.8–1 TPa and ≈ 30 GPa, respectively. The low values observed for N-doped nanotubes are probably the result of the relatively high N concentration (*e.g.*, 2–5 %) within the tubes, which introduces defects and lowers the mechanical strength.[26]

Recent results showed that CNTs exhibit virtually no fatigue.[48] A 2 mm square block of vertically aligned, multi-walled nanotubes still retains its original structural integrity and properties after being compressed and released more than 500,000 times. The results show that the ability of CNTs to resist wear and tear is similar to the behaviour of muscles, stomach lining, and other soft tissues. This ability, coupled with the strong electrical conductivity of CNTs, suggests that they could be used to create artificial muscles.

4.4. Thermal properties

Although the thermal properties of carbon nanotubes, including their specific heat, thermal conductivity, and thermopower, are quite special, the thermal properties of SWNTs have not been as extensively studied as the electronic, mechanical, or phonon properties of SWNTs, in part because the techniques for making such studies are still under development. The thermal properties of carbon nanotubes display a wide range of behaviours that stem from their relation to the corresponding properties of a two-dimensional graphene layer and from their unique structure and tiny size.[35]

At high temperatures, the specific heat of individual nanotubes should be similar to that of two-dimensional graphene, with the effects of phonon quantization becoming apparent at lower temperatures for SWNTs of small diameter (< 2 nm), where a linear T-dependence of the specific heat is expected. To study

the intrinsic thermal conductivity and thermoelectric power of nanotubes, measurements must be made at the single nanotube level. Such measurements are technically very difficult to realise. Therefore, work in this area is just beginning to appear in the literature.

The thermal conductivity of graphite is generally dominated by phonons and is limited by the small crystallite size within a sample. The apparent long-range crystallinity of nanotubes and the long phonon mean free path led to the speculation that their longitudinal thermal conductivity could possibly exceed the in-plane thermal conductivity of graphite, which, together with diamond, has the highest thermal conductivity of known materials. The reason for the very high thermal conductivity follows from the very high velocity of sound based on kinetic theory arguments and relates to the very high Young's modulus of carbon nanotubes. From the viewpoint of application, it is important that nanotubes have a high thermal conductivity and can conduct heat efficiently, which would prevent structural damage while used as current-carrying wires in micro/nano devices.

Measurements of the temperature-dependent thermal conductivity $\kappa(T)$ for an individual MWNT (14 nm diameter)[49] show very high values of κ (more than 3000 W m K^{-1}), comparable to graphite (in-plane). It is believed that smaller diameter tubes (probably individual SWNTs) will be needed to exhibit thermal conductivities greater than that of graphite. The small diameter of SWNTs causes phonon quantization, which should be observable in the heat capacity and in the thermal conductivity at low T.

The thermal expansion of a SWNT bundle was measured using X-ray diffraction techniques,[50] and the results are consistent with expectations based on graphite. The measurements showed a very small negative thermal expansion along the nanotube axis direction ($-0.15\pm0.20\times10^{-5}$ K^{-1}) but a value of $0.75\pm\pm0.25\times10^{-5}$ K^{-1} was found for the expansion along the of the diameter direction of the SWNT in the temperature range 300–950 K.

Thermopower (TEP) measurements have been of substantial interest in nanotube research. However, most TEP measurements were performed on SWNT bundles with random orientations leading to phenomena dominated by intertube interactions, rather than the intrinsic behaviour of individual SWNTs.

Thermal measurements at the individual nanotube level are expected to have a major impact on the direction of future studies on the thermal properties of nanotubes.

5. APPLICATIONS OF CARBON NANOTUBES

The ultimate electronic device miniaturization would be to use individual molecules as functional devices. Single-wall carbon nanotubes are promising candidates for achieving this. Depending on their diameter and helicity, they are either one-dimensional metals or semiconductors. As already mentioned, they can

therefore be used to form metal–semiconductor, semiconductor–semiconductor, or metal–metal junctions.

Several major steps toward nanotube-based circuitry have been achieved: single-electron transistors employing metallic nanotubes have been demonstrated. An array of field-effect transistors has been made by selectively burning-off metallic nanotubes in SWNT ropes, and several research groups have assembled field-effect transistors based on single nanotubes into logic circuits, which are the building blocks of computers, showing promise for future developments in nanocircuitry.[35]

Intramolecular devices have also been proposed which should display a range of other device functions. For example, by introducing a pentagon and a heptagon into the hexagonal carbon lattice, two tube segments with different atomic and electronic structures can be seamlessly fused together to create intramolecular metal–metal, metal–semiconductor, or semiconductor–semiconductor junctions. Both the existence of such atomic-level structures and investigations of their respective electronic properties have already been carried out experimentally.[51,52]

Joining a semiconducting nanotube to a metallic one, using a pentagon–heptagon pair incorporated in the hexagonal network can be the basis of a nanodiode (or molecular diode) for nano-electronics. An example of such a diode structure is the junction of a semiconducting (8,0) nanotube, which has a 1.2 eV gap in the tight-binding approximation, and a metallic (7,1) tube (although a small curvature-induced gap is present close to the Fermi energy). Nanotube junctions can thus behave as nanoscale metal-metal junctions, metal-semiconductor Schottky barrier junctions, or semiconductor heterojunctions with novel properties, and these different types of junctions can serve as building blocks for nanoscale electronic devices.[35]

A SWNT *p–n* junction diode device has recently been demonstrated.[53] The *p–n* junction was formed along a single nanotube by electrostatic doping using a pair of split gate electrodes. The device can function either as a diode or as an ambipolar field-effect transistor.

An interesting recent development is the employment of the electron beam of a transmission electron microscope to covalently connect crossed SWNTs, which can be useful for device applications. Electron beam welding at elevated temperatures was used to produce molecular junctions of various geometries ("X," "Y," and "T" junctions) and these junctions were found to be stable after the irradiation process. To study the relevance of some of these nanostructures, various models of ideal molecular junctions were generated. The presence of heptagons plays a key role in the topology of nanotube-based molecular junctions. The flexibility of the nanoscale design and the availability of both semiconducting and metallic nanotubes enable a wide variety of configurations. Junctions between semiconducting and metallic nanotubes can act as diodes. Junc-

tions between two crossed nanotubes can act as rectifiers and Y-, T-, or X-junctions and provide more exotic configurations for nanoscale devices.[54]

Another recent publication[55] describes the fabrication of ultrathin, transparent, optically homogeneous, electrically conducting films of pure single-walled carbon nanotubes and the transfer of these films to various substrates, in order to extend the application of CNTs in electronics.

A number of potential applications arise if, instead of undoped CNTs, B- or N-doped nanotubes are used. Theoretical calculations and experimental results[56] have shown that B-doped MWNTs could exhibit enhanced field emission (turn-on voltages of ≈ 1.4 V μm^{-1}) when compared to pristine carbon MWNTs (turn-on voltages of ≈ 3 V μm^{-1}). This phenomenon arises from the preferential presence of B atoms at the nanotube tips, which results in an increased density of states close to the Fermi level. Similarly, Golberg *et al.*[57] demonstrated that N-doped MWNTs are able to emit electrons at relatively low turn-on voltages (2 V μm^{-1}) and high current densities (0.2–0.4 A cm^{-2}). More recently, it was found[26] that individual N-doped MWNTs exhibit excellent field emission properties at 800 K: experimental work functions of 5 eV and emission currents of ≈ 100 nA were obtained at ±10 V. One of the first demonstrated applications was intense electron emitters for large displays, with the metal tips replaced by CNTs. The improvements were a clearer picture, longer life of the emitter and a simpler device, which need neither ultrahigh vacuum nor high temperature (the CNTs emit electrons at room temperature).

Thus, both B- and N-doped CNTs may have great potential as building blocks for stable and intense field-emission sources.

The next application involves the well-known Li^+ batteries (with the Li^+ ions intercalated between the layers in graphite) used for portable computers, mobile telephones, digital cameras, *etc*. If instead of graphite, N-doped CNTs are used, much higher energy storage (480 mA h g^{-1}) will be achieved than in commercial carbon materials used for Li^+ batteries (330 mA h g^{-1}). Interestingly, such nanotubes consist of many short segments with one end closed and the other one open. Upon Li^+ intercalation into the N-doped MWNTs, the graphene layers (the number of which is several tens) expanded and become partly disordered, while after deintercalation, they reorder to a certain degree.[58]

An important application from the ecological viewpoint is for sensors detecting hazardous gases. The N-doped MWNTs have proved more efficient than pure SWNTs or MWNTs, displaying a fast response in the order of milliseconds when exposed to toxic gases and organic solvents, reaching saturation within 2–3 s. Furthermore, while CO and H_2O molecules apparently do not react with the surface of pure carbon SWNTs, if the surface of the tube was doped with a donor or an acceptor, drastic changes in the electronic properties were observed as a result of the binding of the molecules to the doped locations.[26]

An obvious potential application of the CNTs is to reinforce plastic-based composites. The huge strength and modulus values found (see 4.3. Mechanical properties) indicate that composites with CNT reinforcement should have much higher mechanical properties than any other material known. In principle, the preference is to use single-walled tubes for making composites, because the inner layers of multi-walled tubes probably contribute little to the carrying load.

Standard composites with continuous-carbon-fibre reinforcement have excellent stiffness and strength combined with low density, but are expensive to process and are limited to simple shapes, such as sheets and tubes. Short fibre composites, on the other hand, can be moulded, but the fibres become chopped down to a maximum length of about 1 mm during the processing. At this length, the aspect ratio is only about 100, which is not enough to make an extremely strong material. Nanotubes can have aspect ratios of 1,000 or more, and hence, in theory, they should make excellent composites.

However, experiments intended to make strong composites with CNTs have been unsuccessful.[59] The main reason is that highly crystalline CNTs tend to be similar to graphite, and chemically "inert", and it is, therefore, necessary to modify their surface so that efficient tube–matrix interactions can be achieved. The doping with silicon seems to offer a possible solution to this problem,[9] because Si tends to form sp^3 bonds, thus increasing the reactivity of the CNT surface. This, however, remains to be experimentally verified.

The creation of nanotubes containing a few foreign atoms, such as N or B, in the hexagonal network could also circumvent the problem of the non-reactivity of the surface of CNTs. The mechanical properties of the CNTs would not be significantly changed if the dopant concentration were low. Nevertheless, not many experiments have been made so far and much further work is required to solve the problem of fabricating CNT-reinforced plastic matrix composites in a way suitable for commercial production.[26]

Other possible mentioned usages of nanotubes[56] are STM and AFM tips, gas storage devices, actuators, high power electrochemical capacitors, nanothermometers, Fe-filled nanotubes as magnetic storage devices, *etc*. Thus, although a number of early nanotube-based devices have already been demonstrated, the production and integration of nanotube components into reproducible device structures still present many challenges.

Of particular interest is research aimed at merging biotechnology with materials (especially nanomaterials) science. This will allow not only the advantage of improved evolutionary biological components to be taken to generate new smart materials but also to apply today's characterization and fabrication techniques of advanced materials to solving biological problems. Carbon nanotubes functionalized with biological molecules (such as protein peptides and nucleic acids) show great potential for application in bioengineering and nanotechnology.

A fundamental understanding, description, and regulation of such bio-nanosystems will ultimately lead to a new generation of integrated systems combining the unique properties of the carbon nanotube with biological recognition capabilities.[60] A recent article[61] describes a developed multi-step method to covalently link DNA with functionalized MWNTs.

The considerable progress in research concerned with CNTs has further increased their potential in biological and biomedical applications.[62] The recent expansion and availability of chemical modification and bio-functionalization methods have enabled the generation of a new class of bioactive carbon nanotubes which are conjugated with proteins, carbohydrates, or nucleic acids. The final aim is to target and to alter the behaviour of cells at the subcellular or molecular level. Current research topics aim at translating biotechnology modified nanotubes into potential novel therapeutic approaches.

Although the list of potential applications of CNTs is rather impressive, the actual practice restrains it to a few issues. The electronic applications seem to be the most important, but numerous problems must be solved. These involve control of helicity, structure and length, but more fundamental studies are also required, such as growth mechanisms of CNTs. According to some predictions,[63] the scaling of microelectronic devices could lead to the utilization of carbon nanotubes in about ten years. Among the applications already developing are field emission displays, field-effect transistors, atomic-force microscope probe tips, interconnects in advanced CMOS manufacture. Some encouraging data are that a process for fabricating CNTs at room temperature has been developed, and its first commercial appearance has already occurred (in 2007).[64]

6. CONCLUDING REMARKS

With diameters of down to 0.4 nm, only one atom in thickness, and length of up to many microns, carbon nanotubes (CNTs) represent a prototype of a one-dimensional (1-D) system. In addition, depending on their diameter and helicity, CNTs are either 1-D metals or large-gap semiconductors. Due to the unique properties of CNTs, there are great expectations that their practical applications will eventually be developed. In addition, they will be used for further theoretical and experimental studies.

The original difficulties in the synthesis of sufficient quantities of pure and well-characterized CNTs for detailed, systematic experimental investigations have largely been overcome. However, due to experimental difficulties, much remains to be performed in the study of their properties.

B- or N-doped CNTs, SWNTs in particular, should exhibit novel electronic, chemical, and mechanical properties that are not found in their pure carbon counterparts, and are likely to become more useful than undoped material. This is particularly true for low concentrations of the dopants (*e.g.*, < 0.5 %), because in this

case the conductance should be significantly enhanced and the mechanical properties would not be significantly altered. In addition, because of the presence of holes (B-doped tubes) or donors (N-doped tubes), their surface should become more reactive, which would be extremely useful in the development of field-emission sources, nanoelectronics, sensors, and strong composite materials. Unfortunately, efficient routes to dope SWNTs are still awaiting development.

It is worth mentioning that substitutional dopants other than B and N also deserve attention. This is true not only for P (donor), but also for Si, in view of their respective effects in pyrolytic carbon (see for example Ref. 65).

Acknowledgment. The author expresses his thanks to B. Djurašević (Vinča Institute of Nuclear Sciences, Belgrade, Serbia) for his help in providing the necessary literature.

И З В О Д

УГЉЕНИЧНЕ НАНОЦЕВИ

СЛОБОДАН Н. МАРИНКОВИЋ

Институт за нуклеарне науке "Винча", п. пр. 522, 11000 Београд

Иако откривене пре више од пола века, угљеничне наноцеви су доспеле у жижу интересовања научне јавности тек после поновног "открића" 1991. године. Овај до скора непознат, ванредно занимљиви облик елементарног угљеника, надовезује се на низ других угљеничних материјала откривених током последњих деценија, који су у знатној мери омогућили развој високе технологије, али и изменили наш свакодневни живот. У овом прегледу је сажето приказано обимно, мада још недовољно знање о угљеничним наноцевима, стечено у току последњих петнаестак година. Обухваћене су методе синтезе, математички опис, карактеризација Раманском спектроскопијом. Најважнија својства и примене. Наведени су проблеми у вези са одређивањем својстава наноцеви, као и тешкоће везане за њихову примену, нарочито преношење технологије производње на (полу)индустријски ниво.

(Примљено 14. марта, ревидирано 17. маја 2008)

REFERENCES

1. L. V. Radushkevich, V. M. Lukyanovich, *Zhurn. Fizich. Khim*. **26** (1952) 88 (in Russian)
2. M. Monthioux, V. L. Kuznetsov, *Carbon* **44** (2006) 1621
3. J. W. Mintmire, B. I. Dunlap, C. T. White, *Phys. Rev. Lett*. **68** (1992) 631
4. S. Iijima, *Nature* **354** (1991) 56
5. T. W. Ebbesen, *Phys. Today* **49** (1996) 26
6. S. lijima, T. Ichihashi, *Nature* **363** (1993) 603
7. D.S. Bethune, C.H. Klang, M.S. deVries, G. Gorman, R. Savoy, J. Vazquez, R. Beyers, *Nature* **363** (1993) 605
8. W. Krätschmer, in *Fullerenes and Nanotubes – An Introduction*, Hans Kuzmany, Ed., *Conference Proceeding* **544** (2000) 3, American Institute of Physics, Melville, NY, USA
9. C. X. Song, Z. Yueyuan, L. Mingwen, L. Xiangdong, H. Feng, Z. Boda, B. Hongyu Zhang, *Phys. Lett. A* **358** (2006) 166
10. P. Chen, X. Wu, J. Lin, K. L. Tan, *Science* **285** (1999) 91

11. S. Eisebitt, A. Karl, A. Zimina, R. Scherer, M. Freiwald, W. Eberhardt, F. Hauke, A. Hirsch, Y. Achiba, *AIP Conf. Proc*. **544** (2000) 380
12. X. Liu, T. Pichler, M. Knupfer, M. S. Golden, J. Fink, H. Kataura, *AIP Conf. Proc*. **633** (2002) 267
13. N. M. Nemes, J. E. Fischer, K. Kamaras, D. B. Tanner, A. G. Rinzler, *AIP Conf. Proc.* **633** (2002) 259
14. H. Rauf, T. Pichler, F. Simon, H. Kuzmany, *AIP Conf. Proc*. **723** (2004) 213
15. T. Pichler, H. Rauf, M. Knupfer, J. Fink, H. Kataura, *Synth. Met.* **153** (2005) 333
16. P. Petit, E. Jouguelet, C. Mathis, P. Bernier, *AIP Conf. Proc*. **544** (2000) 395
17. L. Petaccia, A. Goldoni, S. Lizzit, R. Larciprete, *J. El. Spectr. Relat. Phenom*. **144–147** (2005) 793
18. X. Liu, T. Pichler, M. Knupfer, J. Fink, *AIP Conf. Proc*. **723** (2004) 205
19. A. M. Rao, P. C. Eklund, S. Bandow, A. Thess, R. E. Smalley, *Nature* **388** (1997) 257
20. L. Grigorian,, S. Colbern, I. O. Maciel, M. A. Pimenta, F. Plentz, A. Jorio, *Nanotechnology* **18** (2007) 435705
21. X. Fan, E. C. Dickey, P. C. Eklund, K. A. Williams, L. Grigorian, R. Buczko, S. T. Pantelides, S. J. Pennycook, *Phys. Rev. Lett.* **84** (2000) 4621
22. L. Grigorian, K. A. Williams, S. Fang, G. U. Sumanasekera, A. L. Loper, E. C. Dickey, S. J. Pennycook, P. C. Eklund, *Phys. Rev. Lett.* **80** (1998) 5560
23. N. Bendiab, R. Almairac, S. Rols, R. Aznar, J.-L. Sauvajol, I. Mirebeau, *Phys. Rev. B* **69** (2004) 195415
24. M. Monthioux, *Carbon* **40** (2002) 1809
25. T. W. Ebbesen, P. M. Ajayan, *Nature* **358** (1992) 220
26. M. Terrones, A. Jorio, M. Endo, A. M. Rao, Y. A. Kim, T. Hayashi, H. Terrones, J.-C. Charlier, G. Dresselhaus, M. S. Dresselhaus, *Mater. Today* **7(10)** (2004) 30
27. M. Glerup, J. Steinmetz, D. Samaille, O. Stephan, S. Enouz, A. Loiseau, S. Roth, P. Bernier, *Chem. Phys. Lett.* **387** (2004) 193
28. A. Thess, R. Lee, *Science* **273** (1996) 483
29. Y. Zhang, H. Gu, K. Suenaga, S. Iijima, *Chem. Phys. Lett*. **279** (1997) 264
30. P. L. Gai, O. Stephan, K. McGuire, A. M. Rao, M. S. Dresselhaus, G. Dresselhaus, C. Colliex, *J. Mater. Chem*. **14** (2004) 669
31. E. Borowiak-Palen, T. Pichler, G. G. Fuentes, A. Graff, R. J. Kalenczuk, M. Knupfer, J. Fink, *Chem. Phys. Lett*. **378** (2003) 516
32. R. Saito, M. Fujita, G. Dresselhaus, M. S. Dresselhaus, *Appl. Phys. Lett.* **60** (1992) 2204
33. K. Hata, D. N. Futaba, K. Mizuno, T. Namai, M. Yumura, S. Iijima, *Science* **306** (2004) 1362
34. M. J. Height, J. B. Howard, J. W. Tester, J. B. Vander Sande, *Carbon* **42** (2004) 2295
35. M. S. Dresselhaus, G. Dresselhaus, A. Jorio, *Annu. Rev. Mater. Res*. **34** (2004) 247
36. A. M. Rao, E. Richter, S. Bandow, B. Chase, P. C. Eklund, K. A. Williams, S. Fang, K. R. Subbaswamy, M. Menon, A. Thess, R. E. Smalley, G. Dresselhaus, M. S. Dresselhaus, *Science* **275** (1997) 187
37. A. Jorio, R. Saito, J. H. Hafner, C. M. Lieber, M. Hunter, T. McClure, G. Dresselhaus, M. S. Dresselhaus, *Phys. Rev. Lett*. **86** (2001) 1118
38. Ge. G. Samsonidze, R. Saito, A. Jorio, A. G. Souza Filho, A. Grüneis, M. A. Pimenta, G. Dresselhaus, M. S. Dresselhaus, *Phys. Rev. Lett*. **90** (2003) 027403
39. N. Wang, Z. K. Tang, G. D. Li, J. S. Chen, *Nature* **408** (2000) 50

40. Z. K. Tang, L. Zhang, N. Wang, X. X. Zhang, G. H. Wen, G. D. Li, J. N. Wang, C. T. Chan, P. Sheng, *Science* **292** (2001) 2462
41. S. Latil, S. Roche, D. Mayou, J.-C. Charlier, *Phys. Rev. Lett.* **92** (2004) 256805
42. D. Golberg, Y. Bando, L. Bourgeois, K. Kurashima, T. Sato, *Carbon* **38** (2000) 2017
43. M. R. Falvo, G. J. Clary, R. M. Taylor, V. Chi, F. P. Brooks Jr., S. Washburn, R. Superfine, *Nature* **389** (1997) 582
44. M.-F. Yu, B. S. Files, S. Arepalli, R. S. Ruoff, *Phys. Rev. Lett*. **84** (2000) 5552
45. P. Poncharal, Z. L. Wang, D. Ugarte, W. A. de Heer, *Science* **283** (1999) 1513
46. E. Hernández, C. Goze, P. Bernier, A. Rubio, *Phys. Rev. Lett*. **80** (1998) 4502
47. E. Hernández, C. Goze, P. Bernier, A. Rubio, *Appl. Phys*. *A* **68** (1999) 287
48. C. Reinhold, *Mater. Today* **10(9)** (2007) 10
49. J. P. Small, L. Shi, P. Kim, *Solid State Commun*. **127** (2003) 181
50. Y. Maniwa, R. Fujiwara, H. Kira, H. Tou, H. Kataura, S. Suzuki, Y. Achiba, E. Nishibori, M. Takata, M. Sakata, A. Fujiwara, H. Suematsu, *Phys. Rev*. *B* **64** (2001) 241402
51. Z. Yao, H. W. Ch. Postma, L. Balents, C. Dekker, *Nature* **402** (1999) 273
52. M. Ouyang, J.-L. Huang, C. L. Cheung, C. M. Lieber, *Science* **292** (2001) 702
53. J. U. Lee, P. P. Gipp, C. M. Heller, *Appl. Phys. Lett***. 85** (2004) 145
54. M. Terrones, F. Banhart, N. Grobert, J.-C. Charlier, H. Terrones, P. M. Ajayan, *Phys. Rev. Lett*. **89** (2002) 075505
55. Z. Wu, Z. Chen, X. Du, J. M. Logan, J. Sippel, M. Nikolou, K. Kamaras, J. R. Reynolds, D. B. Tanner, A. F. Hebard, A. G. Rinzler, *Science* **305** (2004) 1273
56. J.-C. Charlier, M. Terrones, M. Baxendale, V. Meunier, T. Zacharia, N. L. Rupesinghe, W. K. Hsu, N. Grobert, H. Terrones, G. A. J. Amaratunga, *Nano Lett.* **2** (2002) 1191
57. D. Golberg, P. S. Dorozhkin, Y. Bando, Z.-C. Dong, C. C. Tang, Y. Nemura, N. Grobert, M. Reyes-Reyes, H. Terrones, M. Terrones, *Appl. Phys*., *A* **76** (2003) 499
58. D. Y. Zhong, G. Y. Zhang, S. Liu, E. G. Wang, Q. Wang, H. Li, X. J. Huang, *Appl. Phys. Lett*. **79** (2001) 3500
59. P. Calvert, *Nature* **399** (1999) 210
60. H. Gao, Y. Kong, *Annu. Rev. Mater. Res*. **34** (2004) 123
61. W. Chen, C. H. Tzang, J. Tang, M. Yang, S. T. Lee, *Appl. Phys. Lett*. **86** (2005) 103114
62. W. Yang, P. Thordarson, J. J. Gooding, S. P. Ringer, F. Braet, *Nanotechnology* **18** (2007) 412001
63. J. Robertson, *Mater. Today* **10(1–2)** (2007) 36
64. T. Cheyney, *Small Times,* September 2007
65. S. N. Marinković, in *Chemistry and Physics of Carbon*, Vol. 19, P. A. Thrower, Ed., Marcel Dekker, N.Y., 1984, pp. 1–64.